Spin Polarization and Electronic Structure calculation of Nickel and Co2MnSi thin film interface

[1]Jibon Krishna Modak, [2]Prof. Dr. Ariful Islam Nahid, [3]Konika Rani
[1]Department of Applied Physics Electronic & Communication Engineering, Bangabandhu Sheikh Mujibur Rahman Science and Technology University (BSMRSTU), Gopalganj
[2]Department of Applied Physics and Electronics Engineering, Rajshahi University, Rajshahi
[3]Deparment of Computer Science and Engineering, Delta Computer and Engineering College, Rangpur

Spintronic is an advanced branch of microelectronics based on the transport of electrons spin instead of charge. Spintronic device are superior compare to present electronic devices. Semiconductor based spintronic devices need to combine the magnetic and semiconductor technology. The spin polarization and electronic structure calculation plays an important role in the development of devices. The specific objective of this thesis is to investigated the spin polarization and electronic structure calculation of Heusler alloy/Semiconductor interface. This is very important for efficient spin injection into semiconductor. In broad sense, the research objectives of this thesis are to start and develop research capability in the spintronics researches and to cope with the global standard researcher.

Introduction

Recently, spintronics has become an exciting and rapidly expanding research field in condensed matter physics [1-5]. The technology roadmaps of various developed countries predict that future devices would be spintronic device due to superiority compare to present electronic devices. Thus, it becomes the very hot research field. It is an advanced discipline of microelectronics. The control and manipulation of electron spin is central to spintronics which aims to represent digital information using spin orientation rather than electron charge [3-5]. Such spin based technologies have a profound impact on making devices because of extra degrees of freedom which can give extra functionality and new capabilities. Future anticipated devices based on electron spin have faster switching time and lower power consumption. Till now, all currently available spin-based devices are memory device and sensor [6]. However, progress is going on for spin-based transistor to make novel reconfigurable logic circuits [7]. However, progress is going on for spin-based transistor to make novel reconfigurable logic circuits [7-10].Meanwhile it provides important research subjects in the field of condensed matter physics. In order to fabricate spin-based device, it is necessary to combine the magnetic and semiconductor technology. Although it is difficult, there is good progress in semiconductor based spintronics. The key things for further development are efficient spin injection, transportation and detection. The question is how can the spin current be generated and injected into semiconductor efficiently. Although developed countries researcher has made tremendous progress in this field, developing countries very few researchers are aware of this field. In this paper, the basics of spin current, requirements of efficient spin injection are reviewed. The problems and perils of spin injection and experimental techniques for spin injection are also illustrated.

Background

Half-metallic ferromagnetism was first introduced by de Groot et al. [11] in half-Heusler compound NiMnSb which crystallizes in $C1_b$crystallographic phase. Half metallic compounds are characterized by metallic electronic band structure for majority spins,

while the band structure of minority spins is semiconductor indicating a high spin polarization around Fermi level (*E*F). Consequently, half-metals can conduct a fully spin-polarized current in principal resulting a very large magneto-resistance.100% spin polarization is a hypothetical situation that can be approached in the limit of vanishing temperature and by neglecting spin-orbit effects [12]. These materials play an important role in various spin-dependent electronic applications like spintronics [13, 14], giant magneto-resistance spin valve [15] and spin injection to semiconductors [16–18]. There are several compounds which are predicted to be half-metallic by ab initio calculations [19–23]. The electronic, magnetic and band gap properties of half- and full-Heusler compounds were studied extensively in previous works [24, 25]. The electronic and spin-polarization properties of half-metallic Heusler alloys were also reviewed in a recent ab initio study [26].

Co-based full-Heusler compounds (Co2YZ) in cubic $L2_1$structure, specially Co2MnSi, are the most promising materials for spintronics applications due to high Curie temperature a , wide band gap in minority spins [23] and easy to synthesize experimentally. Co2FeSi is also a very promising material with 1100 K Curie temperature and 6μB magnetic moment [28]. Co-based Heusler compounds were investigated theoretically in view of density functional calculations and most of them are predicted to be half-metallic [21–24, 27, 29, 30]. Specially, Co2MnSi compound was used in production of thin films [31–33] and devices [34, 35] by several groups. The Heusler alloys are considered to be an ideal local moment system [36, 37] and the origin of the half metalicity of these compounds is more complex than in the half-Heusler alloys

due to the presence of the states located entirely at the Co sites [24, 38]. Kurtulus et al. studied the magnetic exchange interactions for a series of Heusler compounds including Co2MnZ (Z = Ga, Si, Ge, Sn) by TB-LMTO-ASA method within LDA formalism [39]. They reported that the pair exchange interaction parameter of Co-Mn is much larger than the others in Co2MnSi and Co-Mn interactions are responsible for the stability of ferromagnetism. The integer magnetic moment is an important characteristic property for these systems in stoichiometric composition. The small deviations from integer magnetic moment lead significant disruptions in half-metallic character by non-zero electronic density of states for minority spins around Fermi level. It is also an important question that in what conditions half-metallic character is322 The European Physical Journal B preserved. Some compounds show half-metallic property in bulk structure, but half-metallism is destroyed when surface effects are taken into account [40]. Hashemifar et al. demonstrated that half-metalicity of Co2MnSi can be preserved by appropriate termination at the (001) surface by ab initio calculations [43]. Ritchie et al. studied the magnetic, structural and transport properties of Co2MnSi and NiMnSb compounds experimentally [44]. They reported relatively low spin polarizations as: ~45% and ~55% together with non-integer saturation magnetic moments 4.02 and 4.78 μB for NiMnSb and Co2MnSi, respectively. They attribute the obtained results to surface effects (e.g., surface segregation) and antisite disorder. For polycrystalline bulk Co2MnSi, there is not any Mn-Si type antisite disorder, but Mn-Co type disorders were observed at a level between 10 and 14% as suggested by neutron-diffraction experiments [45].

Computational Method

At present day, there are various softwares used for the electronic structure calculation. Some well known packages are the following:

1. Quantum ESPRESSO
2. Win2K
3. VASP

Among them Quantum ESPRESSO is one of the most useful method for calculation electronic band structure and density of state. The word ESPRESSO is meaning that "op**E**n-**S**ource **P**ackage for **R**esearch in **E**lectronic **S**tructure, **S**imulation, and **O**ptimization".

What can QUANTUM ESPRESSO do

`PWscf` can currently perform the following kinds of calculations:

- ground-state energy and one-electron (Kohn-Sham) orbitals;
- atomic forces, stresses, and structural optimization;
- molecular dynamics on the ground-state Born-Oppenheimer surface, also with variable cell;
- Macroscopic polarization and finite electric fields via the modern theory of polarization (Berry Phases).
- The modern theory of polarization (Berry Phases).
- Free-energy surface calculation at fixed cell through meta-dynamics, if patched with PLUMED.

All of the above works for both insulators and metals, in any crystal structure, for many exchange-correlation (XC) functionals (including spin polarization, DFT+U, nonlocal VdW function as, hybrid functional), for norm-conserving (Hamann-Schluter-Chiang) PPs (NCPPs) in separable form or Ultrasoft (Vanderbilt) PPs (USPPs) or Projector Augmented Waves (PAW) method. Non-collinear magnetism and spin-orbit interactions are also implemented.

Input data

Input data for the basic codes of the QUANTUM ESPRESSO distribution, `pw.x` and `cp.x`, is organized as several namelists, and followed by other fields introduced by keywords. The namelists are

&CONTROL:	general variables controlling the run
&SYSTEM:	structural information on the system under investigation
&ELECTRONS:	electronic variables: self-consistency, smearing
&IONS (optional):	ionic variables: relaxation, dynamics
&CELL (optional):	variable-cell dynamics
&EE (optional):	for density counter charge electrostatic corrections

Optional name list may be omitted if the calculation to be performed does not require them. This depends on the value of variable calculation in namelist & CONTROL. Most variables in namelists have default values. Only the following variables in &SYSTEM must always be specified:

`ibrav`	(integer)	Bravais-lattice index
`celldm`	(real, dimension 6)	crystallographic constants
`nat`	(integer)	number of atoms in the unit cell
`ntyp`	(integer)	number of types of atoms in the unit cell
`ecutwfc`	(real)	kinetic energy cutoff (Ry) for wave functions.

For metallic systems, you have to specify how metallicity is treated in variable `occupations`. If you choose `occupations='smearing'`, you have to specify the smearing width `degauss` and optionally the smearing type `smearing`. Spin-polarized systems must be treated as metallic system, except the special case of a single k-point, for which occupation numbers can be fixed (`occupations='from input'` and card OCCUPATIONS).

Explanations for the meaning of variables `ibrav` and `cell dm`, as well as on alternative ways to input structural data, are in files `Doc/INPUT_PW.*` (for `pw.x`) and `Doc/INPUT_CP.*` (for `cp.x`). These files are the reference for input data and describe a large number of other variables as well. Almost all variables have default values, which may or may not fit your needs.

After the namelists, you have several fields (``cards'') introduced by keywords with self-explanatory names:

ATOMIC_SPECIES
ATOMIC_POSITIONS
K_POINTS
CELL_PARAMETERS (optional)
OCCUPATIONS (optional)
The keywords may be followed on the same line by an option. Unknown fields (including some that are specific to `CP`) are ignored by `PWscf` (and vice versa, `CP` ignores `PWscf`-specific fields). See the files mentioned above for details on the available ``cards''.

Note about k points: The k-point grid can be either automatically generated or manually provided as a list of k-points and a weight in the Irreducible Brillouin Zone only of the Bravais lattice of the crystal. The code will generate (unless instructed not to do so: see variable `nosym`) all required k-point and weights if the symmetry of the system is lower than the symmetry of the Bravais lattice. The automatic generation of k-points follows the convention of Monkhorst and Pack.

Result and Discussion

Lattice Constant

All physical properties are related to the energies or difference between the total energies. For instantce , the equilibriumlattice constant of a crystal is the lattice constant that minimizes the total energy; surface and defectes of solid adopt the structure that minimizes their correspondig total energy.If total energies can be calculated , any physical property that can be related to a total energy or to a difference between total energies can be determined computationally . For example , to predict the equlibrium lattice constant of a crystal , a series of total-energy calculations are performed to determined the total energy as a fuction of the lattice constant. As shown in fig.1(1) and 4(2).The result are than plotted on a graph of energy versus lattice constant , and a smooth curve is constructed through the points. The theoretical value for the equlibrium lattice constant is the value of the lattice constant at the minimum of this curve . In the fig.4(1), represent the lattice constant versus total energy graph for nickel.

Where nickel lattice constant is = (6.1)*(0.53)
=3.233Å

In the fig.1(2), represent the the lattice constant versus total energy graph for Co_2MnSi.

Where Co_2MnSi lattice constant is
= (10.6)*(0.53)
=5.62Å

This value is nearly of the previous experimental value where previous value is 3.56Å for nickel and 5.65Å for Co_2MnSi.

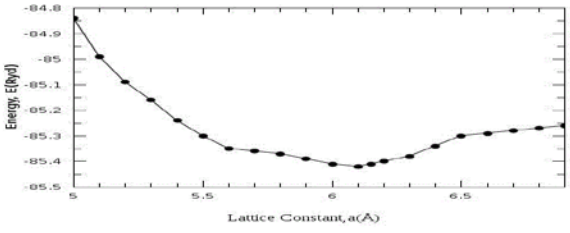

Fig:4.1, Lattice Constant Vs Energy graph for Nickel

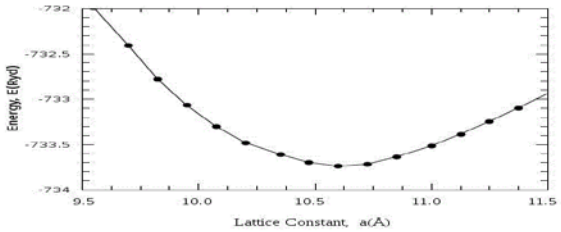

Fig:4.2, Lattice Constant Vs Energy graph for Co_2MnSi

Band Structure of Solid

Any solid has a large number of bands. In theory, a solid can have infinitely many bands (just as an atom has infinitely many energy levels). However, all but a few of these bands lie at energies so high that any electron that attains those energies will escape from the solid. These bands are usually disregarded. Bands have different widths, based upon the properties of the atomic orbitals from which they arise. Also, allowed bands may overlap, producing (for practical purposes) a single large band. Different type of symmetric points is shown in the table 4.1.

Symmetric Points/		
Directions	Coordinate	Remark
Γ	$(0,0,0)$	Origin of **k** space
X	$(1,0,0)$	Middle of square faces
L	$(\frac{1}{2},\frac{1}{2},\frac{1}{2})$	Middle of hexagonal faces
W		Middle of edge shared by two hexagons and a square

Table: 4.1, Different symmetric points.

Ni is a direct band gap material (shown in Fig.4.3). Its primary gap, i.e. minimum gap, is calculated from the valence band maximum at the Γ-point to the conduction band minimum along the Δ direction, 85% of the distance from Γ to X. The band gap of Ni, using the parameters from Ref. [**Error! Bookmark not defined.**], is calculated to be E_g^{Ni} = 0.50 Ryd, in agreement with experimental findings.

Co_2MnSi is also a direct band gap material (shown in Fig.4.3). Its band gap is defined from the top of the valence band at Γ to the conduction band minimum at L. The band gap of Co_2MnSi is calculated to be $E_g^{Co2MnSi}$ = 0.30 Ryd.

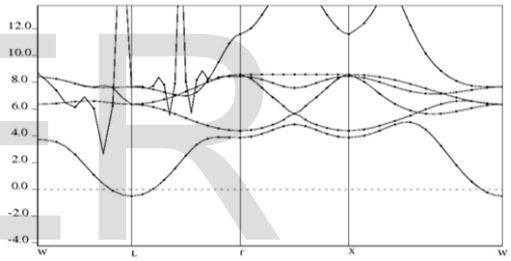

Fig:-4.3, Band structure of Nickel

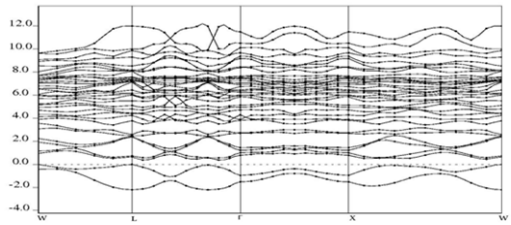

Fig:-4.4, Band structure of Co_2MnSi

Density of State

The term half metallic characterizes a spin-splatted band structure that exhibits different electrical behavior for each spin orientation. In one spin direction (spin up) the conduction electrons exhibit metallic character, where in the opposite spin direction (spin down) semiconducting or insulating behavior is present. This means that the Fermi energy is situated within a gap in the spin down band structure and hence a spin polarization of 100% at the Fermi level exists.

Nickel is a magnetic material. It is also show half metallic properties. From fig.4.5, it can be observed that spin polarization of the nickel is 100%.

Second evidence for the presence of 100% spin polarization was given by theoretical investigations on half Heusler alloys [2]. Co_2MnSi is a half metallic. Initiated by these theoretical findings, numerous experimental studies so as to verify the spin polarization followed. These experiments concentrated on the preparation Co2MnSi of thin films [30, 31, 32, and 33] and to prove their half metallic character, but failed to do so [34, 35, and 36]. As a reason for this failure, two aspects are discussed in literature. Firstly, due to the empty fourth fcc lattice antisite disorder effects are more favored [12, 13].

In the fig.4.6 shown, the two Co-sublattices (one is empty) are indistinguishable. The full Heusler $L2_1$ structure is the more stable phase. And secondly, since in these experiments the spin polarization was determined by surface sensitive techniques (compare also paragraph 3.4), the theoretical predicted missing of half metallicity at the surface [37, 38] can be responsible. Hence full Heusler alloys would be better candidates due to lower tendency to antisite disorder and still half metallic character at the surface/interface for elevated full Heusler alloys [3, 38].

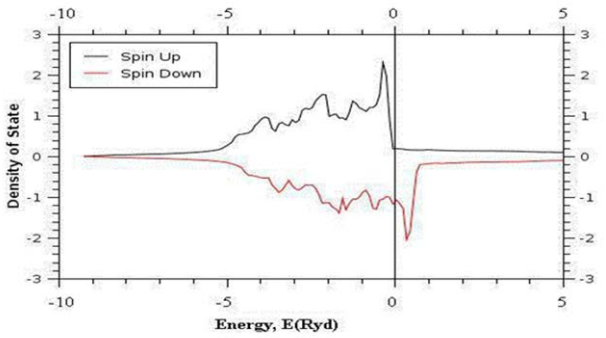

Fig: 4.5, Density of state versus energy curve for Nickel

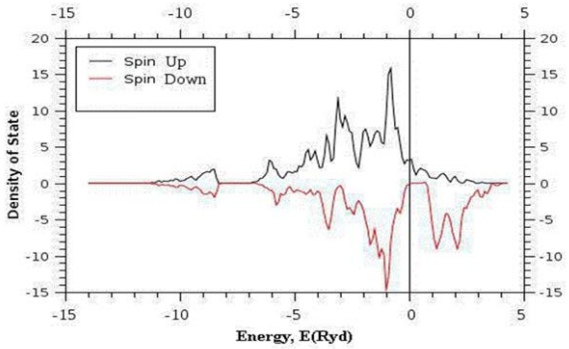

Fig: 4.5, Density of state versus energy curve for Co_2MnSi

Summery and Discussion

In this review we have given an introduction to the electronic structure and the resulting magnetic properties of half-metallic Heusler alloys, which represent interesting hybrids between metallic ferromagnets and semiconductors. First, we reviewed a few recent results on the electronic properties of these alloys. The origin of the gap in these half-metallic alloys and its connection to the magnetic properties are well understood. The gap in half-Heuslers arises between the bonding and antibonding d hybrids created by the transition metal atoms (e.g. Ni and Mn in NiMnSb). In full-Heusler compounds, like Co_2MnSi, there is the extra complication of the appearance of Co d states which do not hybridize with the Mn states. There are exactly nine occupied minority-spin states for the half-Heuslers and 12 for the full-Heuslers; thus the total spin moment follows a Slater–Pauling behaviour for both families. Moderate changes of the lattice parameter shift the Fermi level, but overall do not affect half-metallicity. Spin–orbit coupling also induces states within the gap but the alloys keep a very high degree of spin polarization at the Fermi level. Orbital moments are small, as expected for typical intermetallic ferromagnets.

We discussed the effect of substitutional doping, disorder and defects on the properties of these alloys. In many cases moderate degrees of disorder and doping do not alter half-metallicity. Also, defects with low formation energies, which are the most likely to occur; keep the half-metallic character of the compounds. Quaternary Heusler alloys are a special case of full-Heusler alloys where one site is occupied randomly by two chemical elements. These alloys, when the two extreme normal compounds are half-metallic, follow the Slater–Pauling behavior, keeping the half-metallicity of the normal Heusler alloys. Finally, we discuss the appearance of half-metallic ferrimagnetism in Mn_2VZ (Z and sp element). The results summarized above contribute to the idea that half-metallic ferromagnets are feasible experimentally since all studied effects keep an almost 100% degree of spin polarization at the Fermi level. However, as discussed in the last section, temperature effects quickly destroy the half-metallicity and the alloys transit to a normal metal. Moreover, surfaces/interfaces of Heusler alloys are known from first principles calculations to show strong surface/interface states, which can severely reduce the degree of spin polarization [16, 17]. A theoretical analysis [55] shows that interface states at a half-metal/semiconductor interface can reduce the tunneling magnetoresistance ratio significantly.

In the present work, PWscf method has been employed to study the structural and electronic properties of Nickel and Co2MnSi compounds. The equilibrium lattice constant, band structure and density of state calculated by generalized gradient approximation of density functional theory DFT- GGA. The III-V compounds have been considered in zinc-blend phase defined by their equilibrium lattice constants obtained from the present calculations of total energy minimization. The present DFT-GGA calculations have shown direct band gap structures in zinc-blend phase.

However the conduction band minima of all the above compounds located at - symmetry point, - min, and - X respectively. The energy gaps by the present DFT-GGA calculations for the above cited compounds at high symmetry points is a widely accepted result in the literature for Co2MnSi with DFT-quasi particle (QP) Ref. [86] and non-local EPM calculations is accepted to the present calculation for Co2MnSi . Due to the lack of experimental56 results, the calculated direct band gap value of Nickel and Co2MnSi has been attempted to improve considering the gap value supplied by corrected DFT-GGA calculations given in the literature. In the present DFT calculations, the direct band gap of Nickel and Co_2MnSi is found to be less than the value of the band gap calculated by the same approximation. A small discrepancy is also found between the present and reported valence band width values of BP. But DFT calculations of Nickel of the direct band gap is 0.5Ryd and Co2MnSi of the direct band gap is 0.3Ryd

Bibliography

[1] A. Fert, “The present and the future of spintronics”, *Thin Solid Films* **517**, 2 (2008).
[2] S. A. Wolf et al., “Spintronics: A spin-based electronics vision for the future”, *Science* **294**, 1488 (2001).
[3] S.D. Bader and S. Parkin, “Spintronics”, *Annu. Rev. Condens. Matter Phys.* **1** 3.1, (2010).
[4] J. F. Gregg, I. Petej, E. Jouguelet and C. Dennis, “Spin electronics—a review”, *J. Phys. D: Appl. Phys.* **35**, R121 (2002).
[5] I. Zutic, J. Fabian, C. D. Sarma, “Spintronics: fundamentals and applications”, Rev. Mod. Phys. **76**, 323 (2004).
[6] P. Sharma, “How to create a spin current”, *Science* **307**, 531(2005).
[7] Tanaka, “Spintronics: recent progress and tomorrow’s challenges”, *J. Crystal Growth* **278**, 25 (2005).

[8] K. Takanashi, “Generation and control of spin current in magnetic nanostructures”, *AAPPS Bulletin* **18**, 47 (2008).
[9] B. K. Nikoli´c, L. P. Zˆarbo, and S. Souma, “The Oxford Handbook on Nanoscience and Technology: Frontiers and Advances," *Oxford University Press*, (2010) pp. 814.
[10] N. F. Mott, “The electrical conductivity of transition metals,” *Proc. R. Soc. London, Ser. A* **153**, 699 (1936).
[11] Figure is taken from the presentation of Prof. M. Scheffler in the densityfunctional theory workshop at Los Angeles, (2005).
[12] M. Krause et al., Submitted to Phys. Rev. B.
[13] C. Kittel, *Introduction to Solid State Physics*, 5th ed. (Wiley, New York (1983).
[14] A. G. Beattie and J. E. Schirber, Phys. Rev. B **1**, 1548 (1970).
[15] N. Moll, M. Bockstedte, M. Fuchs, E. Pehlke, and M. Scheffler, Phys. Rev. B **52**, 2550 (1995).
[16] A. A. Stekolnikov and F. Bechstedt, Phys. Rev. B **72**, 125326 (2005).
[17] G. Uhlenbeck and S. Goudsmit, Nature **117**, 264 (1926).
[18] M. N. Baibich et al., Phys. Rev. Lett. **61**, 2472 (1988).
[19] G. Binash, P. Gr¨unberg, F. Saurenbach, and W. Zinn, Phys. Rev. B **39**, 4828 (1989).
[20] J.-P. Ansermet, J. Phys.:Condens. Matter **10**, 6027 (1998).
[21] M. A. M. Gijs and G. E. Bauer, Advances in Physics **46**, 285 (1997).
[22] J. Bass and W. P. Pratt, J. Magn. Magn. Mater. **200**, 274 (1999).
[23] M. Julliere, Phys. Lett. **54A**, 225 (1975).
[24] J. S. Moodera, L. R. Kinder, T.M.Wong, and R. Meservey, Phys. Rev. Lett. **74**, 3273 (1995).
[25] Y. C. Lian and L. J. Chen, Appl. Phys. Lett. **48**, 359 (1986).
[26] H. Lippitz, J. J. Paggel, and P. Fumagalli, Surf. Sci. **575**, 307 (2005).
[27] K. Schwinger, C.M¨ uller, A. Mogilatenko, J. Paggel, and P. Fumagalli, J. Appl. Phys. **97**, 103913 (2005).
28] M. M. R. Evans, J. C. Glueckstein, and J. Nogami, Phys. Rev. B **53**, 4000 (1996).
[29] T. Nagao, S. Ohuchi, Y. Matsuoka, and S. Hasegawa, Surf. Sci. **419**, 134 (1999).
150 Bibliography
[30] G. Ctistis, U. Deffke, J. Paggel, and P. Fumagalli, J. Magn. Magn. Mater. **240**, 420 (2002).
[31] G. Ctistis, U. Deffke, K. Schwinger, J. Paggel, and P. Fumagalli, Phys. Rev. B **71**, 35431 (2005).
[32] A. Kumar, M. Tallarida, M. Hansmann, U. Starke, and K. Horn, J. Phys. D: Appl. Phys. **37**, 1083 (2004).
[33] E. Fermi, Z. Phys. **48**, 73 (1928).
[34] L. H. Thomas, Proc. Cambridge Philos. Soc. **23**, 542 (1927).
[35] P. Hohenberg andW. Kohn, Phys. Rev. **136**, B 864 (1964).
[36] R. O. Jones and O. Gunnarsson, Rev. Mod. Phys. **61**, 689 (1989).
[37] G. P. Parr and W. Yang, *Density-Functional Theory of Atoms and Molecules*, Oxford University Press (1994).
[38] R. M. Dreizler and E. K. U. Gross, *Density Functional Theory*, Springer-Verlag (1990).
[39] W. Kohn and L. J. Sham, Phys. Rev. **140**, A 1133 (1965).
[40] E.Wigner, Phys. Rev. **46**, 1002 (1934).
[41] L. Hedin and B. I. Lundqvist, J. Phys. C **4**, 2064 (1971).
[42] J. P. Perdew and Y.Wang, Phys. Rev. B **45**, 13244 (1992).
[43] D. M. Ceperley and B. J. Adler, Phys. Rev. Lett **45**, 566 (1980).
[44] J. P. Perdew, K. Burke, and M. Ernzerhof, Phys. Rev. Lett **77**, 3865 (1969).
[45] J. C. Slater, Phys. Rev. **51**, 846 (1937).
[46] T. L. Loucks, *Augmeted Plane Wave Method: a guide to performing electronic structure calculations*, Benjamin, New York (1967).